



STRUCTURAL SCIENCE  
CRYSTAL ENGINEERING  
MATERIALS

**Volume 76 (2020)**

**Supporting information for article:**

**The solubility and stability of heterocyclic chalcones compared with *trans*-chalcone**

**Stephen G. Sweeting, Charlie L. Hall, Jason Potticary, Natalie E. Pridmore, Stephen D. Warren, Matthew E. Cremeens, Gemma D. D'Ambruoso, Masaomi Matsumoto and Simon R. Hall**

## Contents of supporting information

### 1- Detailed synthesis of both heterocyclic chalcones

### 2- Solubility data for both heterocyclic chalcones and *trans*-chalcone

**Table S1-** Solubility data for both heterocyclic chalcones and *trans*-chalcone, with solvent properties.

### 3- Nuclear Magnetic Resonance (NMR) data

**Figure S1-** <sup>1</sup>H NMR of (*E*)-1-(1*H*-pyrrol-2-yl)-3-(thiophen-2-yl)prop-2-en-1-one.

**Figure S2-** <sup>13</sup>C NMR of (*E*)-1-(1*H*-pyrrol-2-yl)-3-(thiophen-2-yl)prop-2-en-1-one.

**Figure S3-** <sup>13</sup>C NMR of (*E*)-1-(1*H*-pyrrol-2-yl)-3-(thiophen-2-yl)prop-2-en-1-one in the range 110 – 142 ppm.

**Figure S4-** <sup>1</sup>H NMR of (*E*)-3-phenyl-1-(1*H*-pyrrol-2-yl)prop-2-en-1-one.

**Figure S5-** <sup>13</sup>C NMR of (*E*)-3-phenyl-1-(1*H*-pyrrol-2-yl)prop-2-en-1-one.

**Figure S6-** <sup>13</sup>C NMR of (*E*)-3-phenyl-1-(1*H*-pyrrol-2-yl)prop-2-en-1-one in the range 108 – 180 ppm.

### 4- Crystal growth via slow evaporation

**Figure S7-** Images of (*E*)-1-(1*H*-pyrrol-2-yl)-3-(thiophen-2-yl)prop-2-en-1-one crystals that were grown by the slow evaporation process from a number of different solvents.

**Figure S8-** Images of (*E*)-3-phenyl-1-(1*H*-pyrrol-2-yl)prop-2-en-1-one crystals that were grown by the slow evaporation process from a number of different solvents.

### 5- Molecular electrostatic potential (MEP) plots

**Figure S9-** The MEP's for the three chalcones being considered in the range  $-6.5 \times 10^{-2}$  to  $6.5 \times 10^{-2}$  with an isovalue, MO = 0.020000, density = 0.000400.

### 6- Differential Scanning Calorimetry (DSC)

**Figure S10-** DSC heating and cooling cycle for *trans*-chalcone.

**Figure S11-** DSC heating and cooling cycle for (*E*)-3-phenyl-1-(1*H*-pyrrol-2-yl)prop-2-en-1-one.

**Figure S12-** DSC heating and cooling cycle for (*E*)-1-(1*H*-pyrrol-2-yl)-3-(thiophen-2-yl)prop-2-en-1-one.

### 7- Powder X-ray diffraction data

**Figure S13-** Comparison of the simulated powder X-ray pattern of *trans*-chalcone Form I to experimental data.

**Figure S14-** Powder X-ray diffraction data for *trans*-chalcone Form I in the range 5° 2θ to 20° 2θ with reflections indexed.

**Figure S15-** Powder X-ray diffraction data for *trans*-chalcone Form I in the range 20° 2θ to 35° 2θ with reflections indexed.

**Figure S16-** Powder X-ray diffraction data for *trans*-chalcone Form I in the range 35° 2θ to 50° 2θ with reflections indexed.

**Figure S17-** Comparison of the simulated powder X-ray pattern of *trans*-chalcone Form II to experimental data.

**Figure S18-** Powder X-ray diffraction data for *trans*-chalcone Form II in the range 5° 2θ to 20° 2θ with reflections indexed.

**Figure S19-** Powder X-ray diffraction data for *trans*-chalcone Form II in the range 20° 2θ to 35° 2θ with reflections indexed.

**Figure S20-** Powder X-ray diffraction data for *trans*-chalcone Form II in the range 35° 2θ to 50° 2θ with reflections indexed.

**Figure S21-** Comparison of the simulated powder X-ray pattern of (*E*)-3-phenyl-1-(1*H*-pyrrol-2-yl)prop-2-en-1-one to experimental data.

**Figure S22-** Powder X-ray diffraction data for (*E*)-3-phenyl-1-(1*H*-pyrrol-2-yl)prop-2-en-1-one in the range 5° 2θ to 20° 2θ with reflections indexed.

**Figure S23-** Powder X-ray diffraction data for (*E*)-3-phenyl-1-(1*H*-pyrrol-2-yl)prop-2-en-1-one in the range 20° 2θ to 35° 2θ with reflections indexed.

**Figure S24-** Powder X-ray diffraction data for (*E*)-3-phenyl-1-(1*H*-pyrrol-2-yl)prop-2-en-1-one in the range 35° 2θ to 50° 2θ with reflections indexed.

**Figure S25-** Comparison of the simulated powder X-ray pattern of (*E*)-1-(1*H*-pyrrol-2-yl)-3-(thiophen-2-yl)prop-2-en-1-one to experimental data.

**Figure S26-** Powder X-ray diffraction data for (*E*)-1(1*H*-pyrrol-2-yl)-3-(thiophen-2-yl)prop-2-en-1-one in the range 5° 2θ to 20° 2θ with reflections indexed.

**Figure S27-** Powder X-ray diffraction data for (*E*)-1(1*H*-pyrrol-2-yl)-3-(thiophen-2-yl)prop-2-en-1-one in the range 20° 2θ to 35° 2θ with reflections indexed.

**Figure S28-** Powder X-ray diffraction data for (*E*)-1(1*H*-pyrrol-2-yl)-3-(thiophen-2-yl)prop-2-en-1-one in the range 35° 2θ to 50° 2θ with reflections indexed.

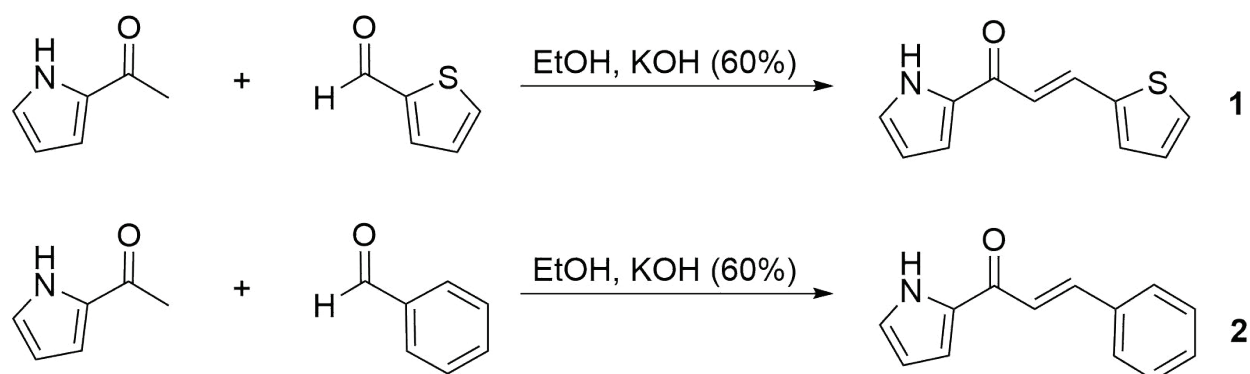
#### **8- Single crystal x-ray diffraction data collected for (*E*)-1-(1*H*-pyrrol-2-yl)-3-(thiophen-2-yl)prop-2-en-1-one.**

**Figure S29-** Labelled diagrams of (*E*)-1(1*H*-pyrrol-2-yl)-3-(thiophen-2-yl)prop-2-en-1-one relating to crystallography data at 50% probability.

**Table S2-** Crystal data and structure refinement relating to (*E*)-1-(1*H*-pyrrol-2-yl)-3-(thiophen-2-yl)prop-2-en-1-one.

**Table S3-** Hydrogen bonds for (*E*)-1-(1*H*-pyrrol-2-yl)-3-(thiophen-2-yl)prop-2-en-1-one.

## 1- Detailed synthesis of both heterocyclic chalcones



2-acetylpyrrole and 2-thiophenylaldehyde were commercially available from TCI and used as obtained. Benzaldehyde was used as obtained from Aldrich. NMR was obtained on a Bruker Advance III HD 400 MHz.

### **(E)-1-(1H-pyrrol-2-yl)-3-(2-thienyl)prop-2-en-1-one**

0.327 g (3.0 mmol) of 2-acetylpyrrole was added to a centrifuge tube containing 1.5 mL of 95% ethanol. 0.28 mL (0.34 g, 3.0 mmol) of 2-thiophenylaldehyde was added to the centrifuge tube. After thorough mixing 0.20 mL of 60% wt/wt KOH (aq) was added to the centrifuge tube. The reaction was allowed to proceed for ~30 minutes with periodic thorough mixing. ~6 mL of ice water was added to the centrifuge tube and mixed followed by the addition of ~6 mL of CH<sub>2</sub>Cl<sub>2</sub>. The tube was thoroughly shaken, and the aqueous layer removed. The organic layer was extracted twice more with ice water. The tube was left uncapped and the CH<sub>2</sub>Cl<sub>2</sub> slowly evaporated over several days to give a solid that was recrystallized out of a minimal amount of hot methanol. 0.140g, 23% yield. <sup>1</sup>H NMR CDCl<sub>3</sub> (**Figure S1**) TMS ref. δ 6.35 (m, 1H), 7.08 (m, 2H), 7.14 (d/m, 2H, J=16 Hz), 7.335 (d, 1H, J=3.5 Hz), 7.395 (d, 1H, J=5 Hz), 7.95 (d, 1H, J=16 Hz), 10.18 (s br, 1H). <sup>13</sup>C NMR, CDCl<sub>3</sub> (**Figure S2 and S3**) ref. δ 111.08, 116.55, 121.12, 125.72, 128.36, 128.42, 131.55, 133.20, 134.85, 140.62, 178.62.

### **(E)-3-phenyl-1-(1H-pyrrol-2-yl)prop-2-en-1-one**

0.327 g (3.0 mmol) of 2-acetylpyrrole was added to a centrifuge tube containing 1.5 mL of 95% ethanol. 0.31 mL (0.34 g, 3.0 mmol) of benzaldehyde was added to the centrifuge tube. After thorough mixing 0.20 mL of 60% wt/wt KOH (aq) was added to the centrifuge tube. The reaction was allowed to proceed for ~30 minutes with periodic thorough mixing. ~6 mL of ice water was added to the centrifuge tube and mixed followed by the addition of ~6 mL of CH<sub>2</sub>Cl<sub>2</sub>. The tube was thoroughly shaken, and the aqueous layer removed. The organic layer was extracted twice more with ice water. The tube was left uncapped and the CH<sub>2</sub>Cl<sub>2</sub> slowly evaporated over several days to give a solid that was recrystallized out of a minimal amount of hot methanol. 0.130g, 22% yield. <sup>1</sup>H NMR CDCl<sub>3</sub> (**Figure S4**) TMS ref. δ 6.36 (m, 1H), 7.09 (s br, 1H), 7.13 (s br, 1H), 7.335 (d/m, 4H, J=16 Hz), 7.64 (m, 2H), 7.84 (d, 1H, J=16 Hz), 9.85 (s br, 1H). <sup>13</sup>C NMR, CDCl<sub>3</sub> (**Figure S5 and S6**) ref. δ 111.15, 116.42, 122.06, 125.50, 128.46, 129.04, 130.36, 133.30, 135.15, 142.42, 178.99

## 2- Solubility data

**Table S1-** Solubility data for both heterocyclic chalcones and *trans*-chalcone, with solvent properties.

Solvent	Nature of solvent	Relative polarity <sup>[a]</sup>	Solubility limit of <i>trans</i> -chalcone / mg ml <sup>-1</sup>	Solubility limit of <b>1</b> / mg ml <sup>-1</sup>	Solubility limit of <b>2</b> / mg ml <sup>-1</sup>
n-Hexane	Non-polar, Aliphatic	0.009	44.0 ± 3.6	Insoluble	Insoluble
Toluene	Non-polar, Aromatic	0.099	630 ± 6.2	Insoluble	14.0 ± 7.1
THF	Polar, aprotic, cyclic	0.207	1010 ± 8.8	213 ± 3.9	105 ± 7.3
Ethyl acetate	Polar, aprotic	0.228	855 ± 7.7	49.5 ± 3.6	49.0 ± 7.1
Chloroform	Polar, aprotic	0.259	730 ± 6.8	65.5 ± 3.6	51.0 ± 7.1
Acetone	Polar, aprotic	0.355	1050 ± 9.1	101 ± 3.6	82.0 ± 7.2
Ethanol	Polar, protic	0.654	175 ± 3.8	9.00 ± 3.5	11.0 ± 7.1
Methanol	Polar, protic	0.762	130 ± 3.7	14.0 ± 3.5	10.5 ± 7.1

[a] The values for relative polarity are normalised from measurements of solvent shifts of absorption (Reichardt and Welton, 2011).

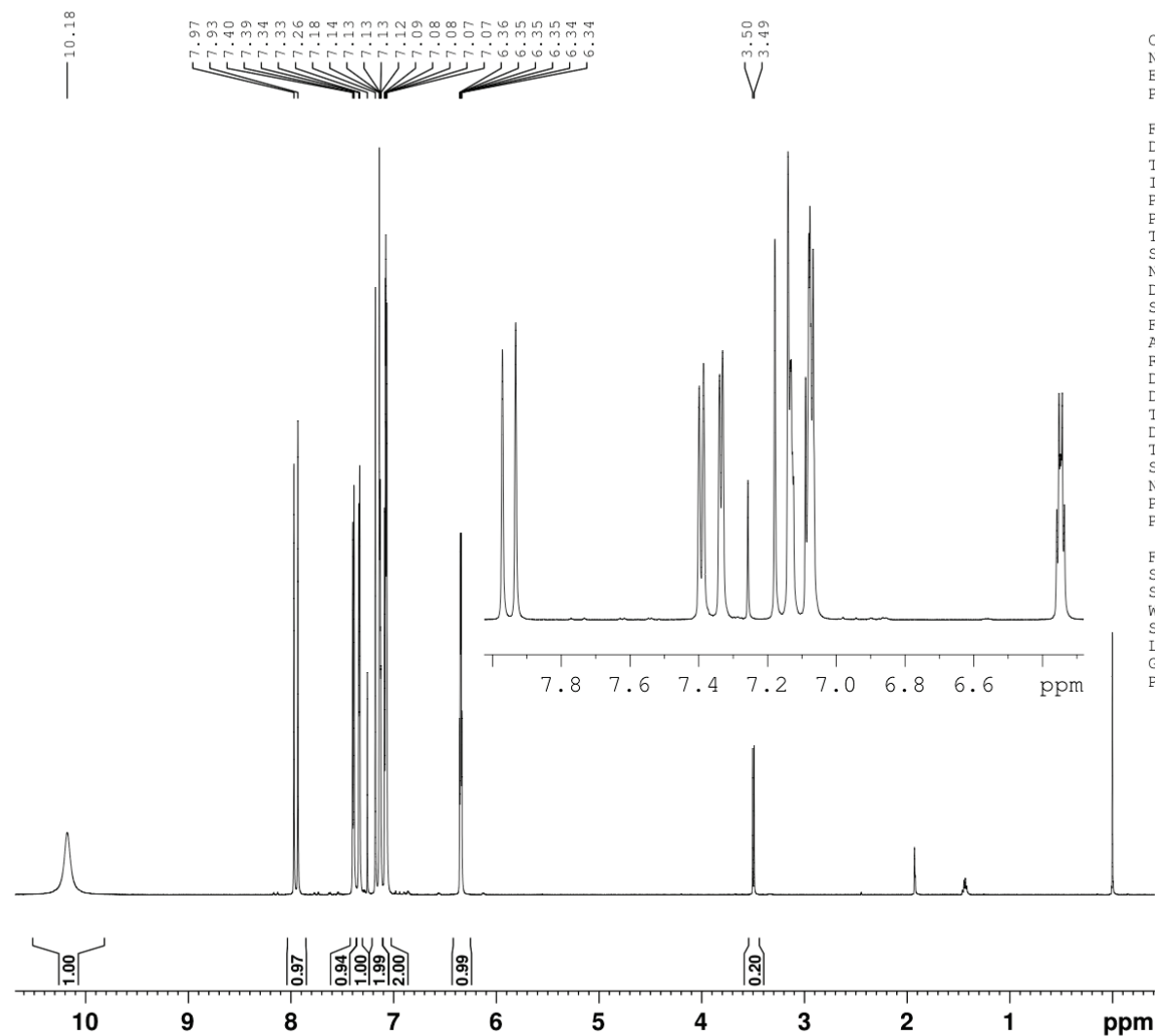
The solvents were chosen to cover a range of different potential interactions that could occur between the chalcones and the solvents. These solvents are also common in most laboratories and are so most likely to be used in the synthesis of more complex molecules where a chalcone is used as a reactant. Values were found by forming saturated solutions of each solvent and chalcone combination, with a volume of either 0.2 cm<sup>3</sup> for *trans*-chalcone and **1**, or 0.05 cm<sup>3</sup> of **2**. Volumes were measured using a Gilson pipette. Different volumes were used due to material availability. Once the saturated solution was formed, the solutions were decanted into pre-weighed test tubes to remove any undissolved chalcone from the solutions. The saturated solutions were left until all the solvent was evaporated. The mass of dissolved chalcone was then recorded and converted into a concentration. Uncertainties for the saturated solution concentrations ( $\delta C$ ) was calculated using the formula:

$$\delta(C) = C \sqrt{\left(\frac{\sqrt{2}(\delta m)^2}{m}\right)^2 + \left(\frac{\delta V}{V}\right)^2}$$

Where  $C$  is the concentration of the saturated solution,  $\delta m$  is the resolution of the balance being used,  $m$  is the mass of the dissolved chalcone,  $\delta V$  is the uncertainty in the Gilson pipette and  $V$  is the volume of solution that was used to form the saturated solution.

### 3- Nuclear Magnetic Resonance (NMR) data

<sup>1</sup>H; Kpr2-Atp2



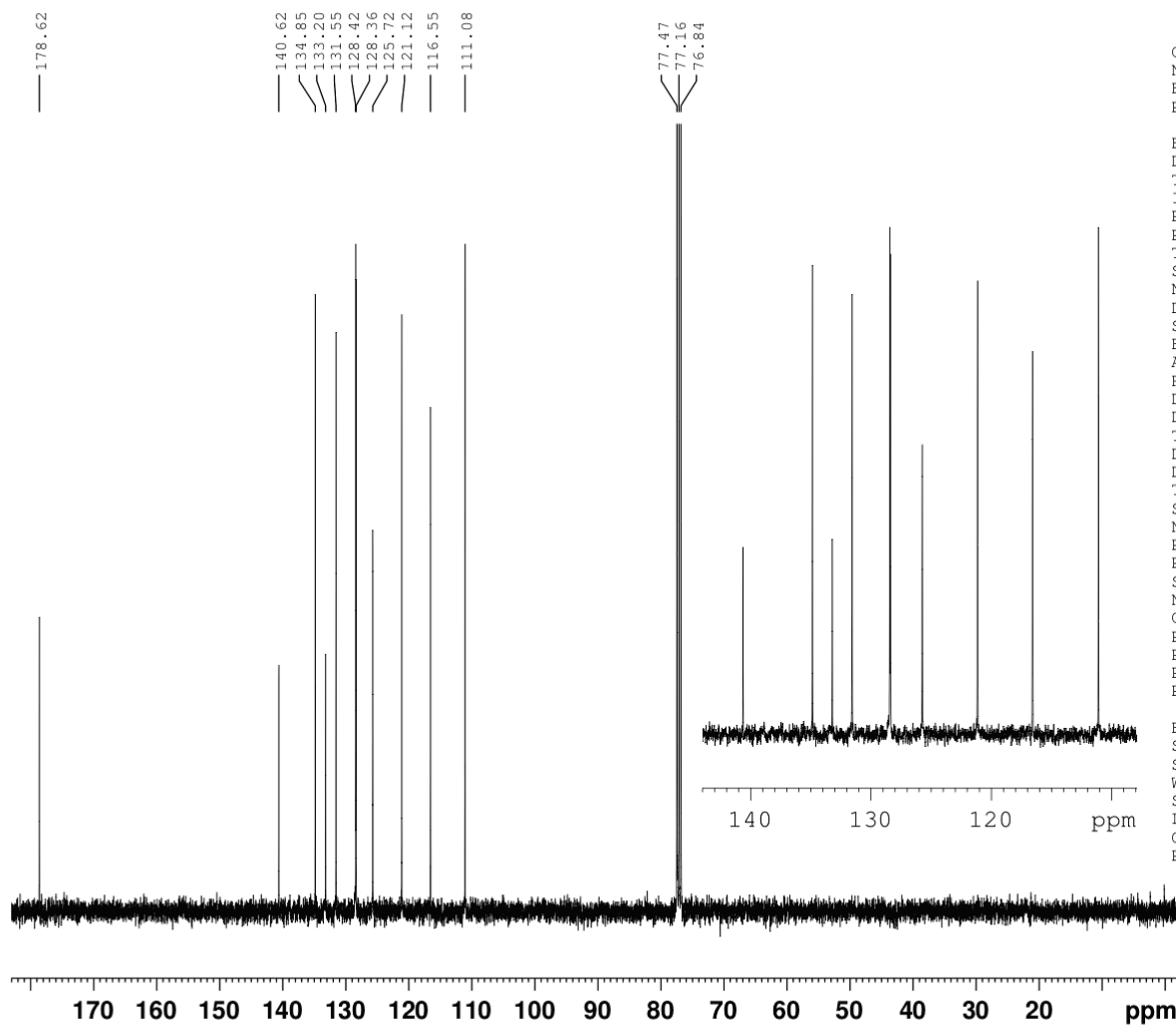
Current Data Parameters  
NAME Kpr2-Atp2  
EXPNO 10  
PROCNO 1

F2 - Acquisition Parameters  
Date\_ 20190604  
Time 16.00 h  
INSTRUM spect  
PROBHD Z108618\_0962 (  
PULPROG zg30  
TD 65536  
SOLVENT CDCl3  
NS 16  
DS 2  
SWH 8012.820 Hz  
FIDRES 0.244532 Hz  
AQ 4.0894465 sec  
RG 126.97  
DW 62.400 usec  
DE 6.50 usec  
TE 294.3 K  
D1 1.00000000 sec  
TD0 1  
SFO1 400.2624716 MHz  
NUC1 1H  
P1 14.00 usec  
PLW1 11.72999954 W

F2 - Processing parameters  
SI 65536  
SF 400.2600111 MHz  
WDW EM  
SSB 0  
LB 0.30 Hz  
GB 0  
PC 1.00

**Figure S1-** <sup>1</sup>H NMR of (*E*)-1-(1*H*-pyrrol-2-yl)-3-(thiophen-2-yl)prop-2-en-1-one.

13C; Kpr2-Atp2



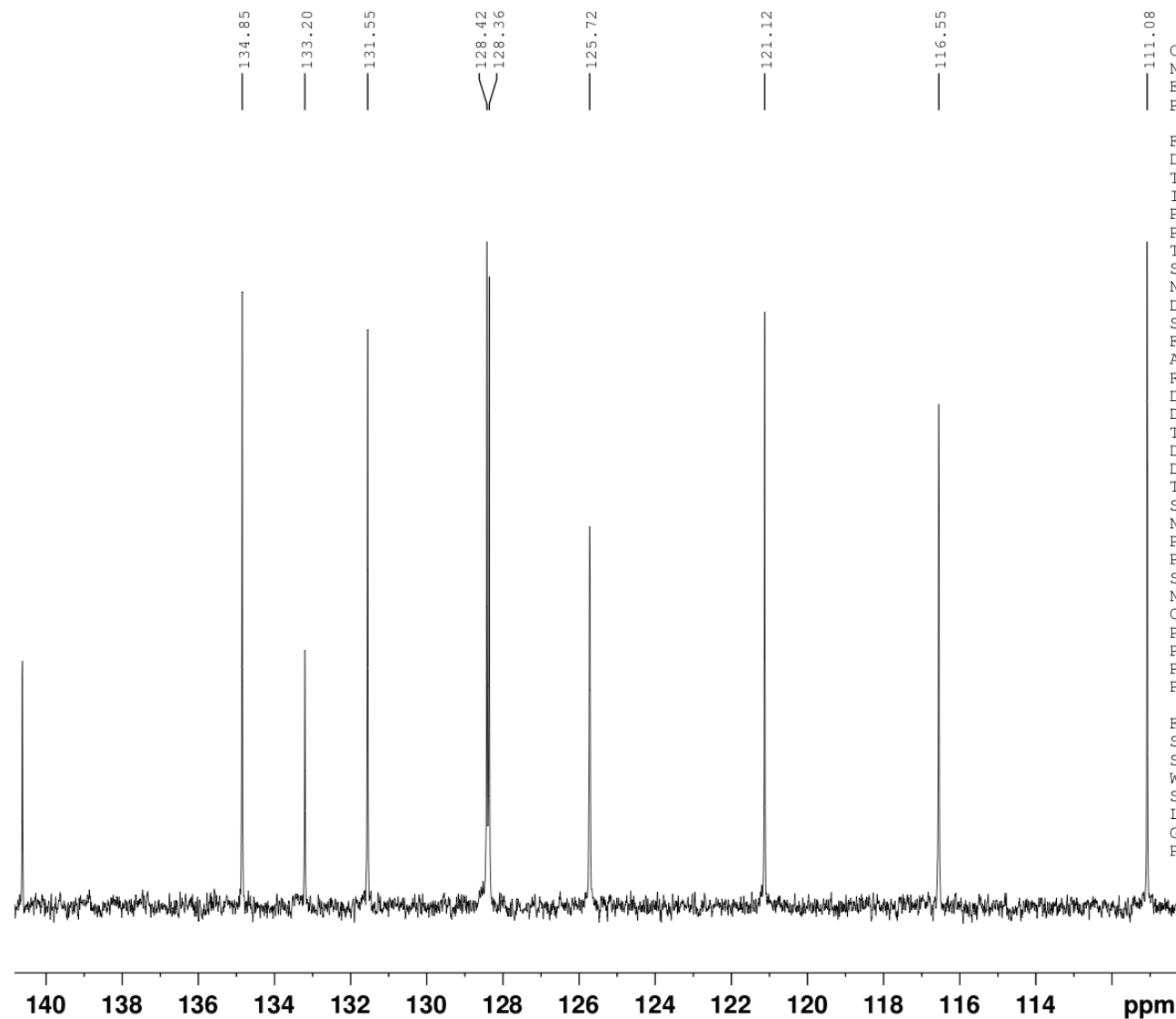
Current Data Parameters  
NAME Kpr2-Atp2  
EXPNO 11  
PROCNO 1

F2 - Acquisition Parameters  
Date\_ 20190604  
Time 16.09 h  
INSTRUM spect  
PROBHD Z108618\_0962 ( )  
PULPROG zgpg30  
TD 65536  
SOLVENT CDCl3  
NS 128  
DS 4  
SWH 24038.461 Hz  
FIDRES 0.733596 Hz  
AQ 1.3631488 sec  
RG 202.4  
DW 20.800 usec  
DE 6.50 usec  
TE 295.2 K  
D1 2.00000000 sec  
D11 0.03000000 sec  
TD0 1  
SFO1 100.6555216 MHz  
NUC1 13C  
P1 10.00 usec  
PLW1 48.63600159 W  
SFO2 400.2616010 MHz  
NUC2 1H  
CPDPRG2 waltz16  
PCPD2 90.00 usec  
PLW2 11.72999954 W  
PLW12 0.28382999 W  
PLW13 0.14275999 W

F2 - Processing parameters  
SI 32768  
SF 100.6454479 MHz  
WDW EM  
SSB 0  
LB 1.00 Hz  
GB 0  
PC 1.40

Figure S2- <sup>13</sup>C NMR of (*E*)-1-(1*H*-pyrrol-2-yl)-3-(thiophen-2-yl)prop-2-en-1-one.

13C; Kpr2-Atp2



Current Data Parameters  
NAME Kpr2-Atp2  
EXPNO 11  
PROCNO 1

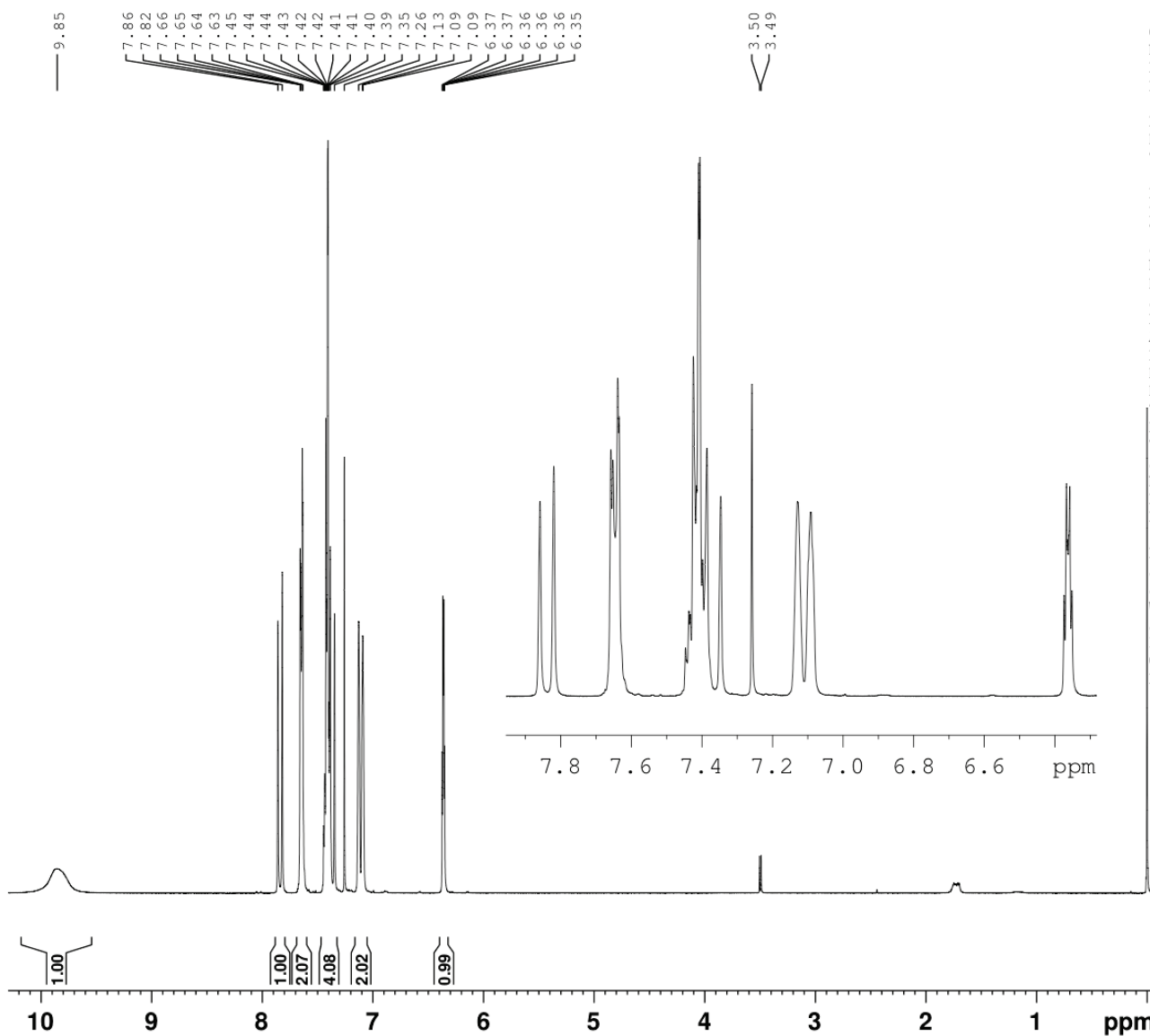
F2 - Acquisition Parameters  
Date\_ 20190604  
Time 16.09 h  
INSTRUM spect  
PROBHD Z108618\_0962 (  
PULPROG zgpg30  
TD 65536  
SOLVENT CDC13  
NS 128  
DS 4  
SWH 24038.461 Hz  
FIDRES 0.733596 Hz  
AQ 1.3631488 sec  
RG 202.4  
DW 20.800 usec  
DE 6.50 usec  
TE 295.2 K  
D1 2.0000000 sec  
D11 0.0300000 sec  
TD0 1  
SFO1 100.6555216 MHz  
NUC1 13C  
P1 10.00 usec  
PLW1 48.63600159 W  
SFO2 400.2616010 MHz  
NUC2 1H  
CPDPRG[2] waltz16  
PCPD2 90.00 usec  
PLW2 11.72999954 W  
PLW12 0.28382999 W  
PLW13 0.14275999 W

F2 - Processing parameters  
SI 32768  
SF 100.6454479 MHz  
WDW EM  
SSB 0  
LB 1.00 Hz  
GB 0  
PC 1.40

Figure S3- <sup>13</sup>C NMR of (*E*)-1-(1*H*-pyrrol-2-yl)-3-(thiophen-2-yl)prop-2-en-1-one in the range 110 – 142 ppm.



1H; Kpr2-Aph1



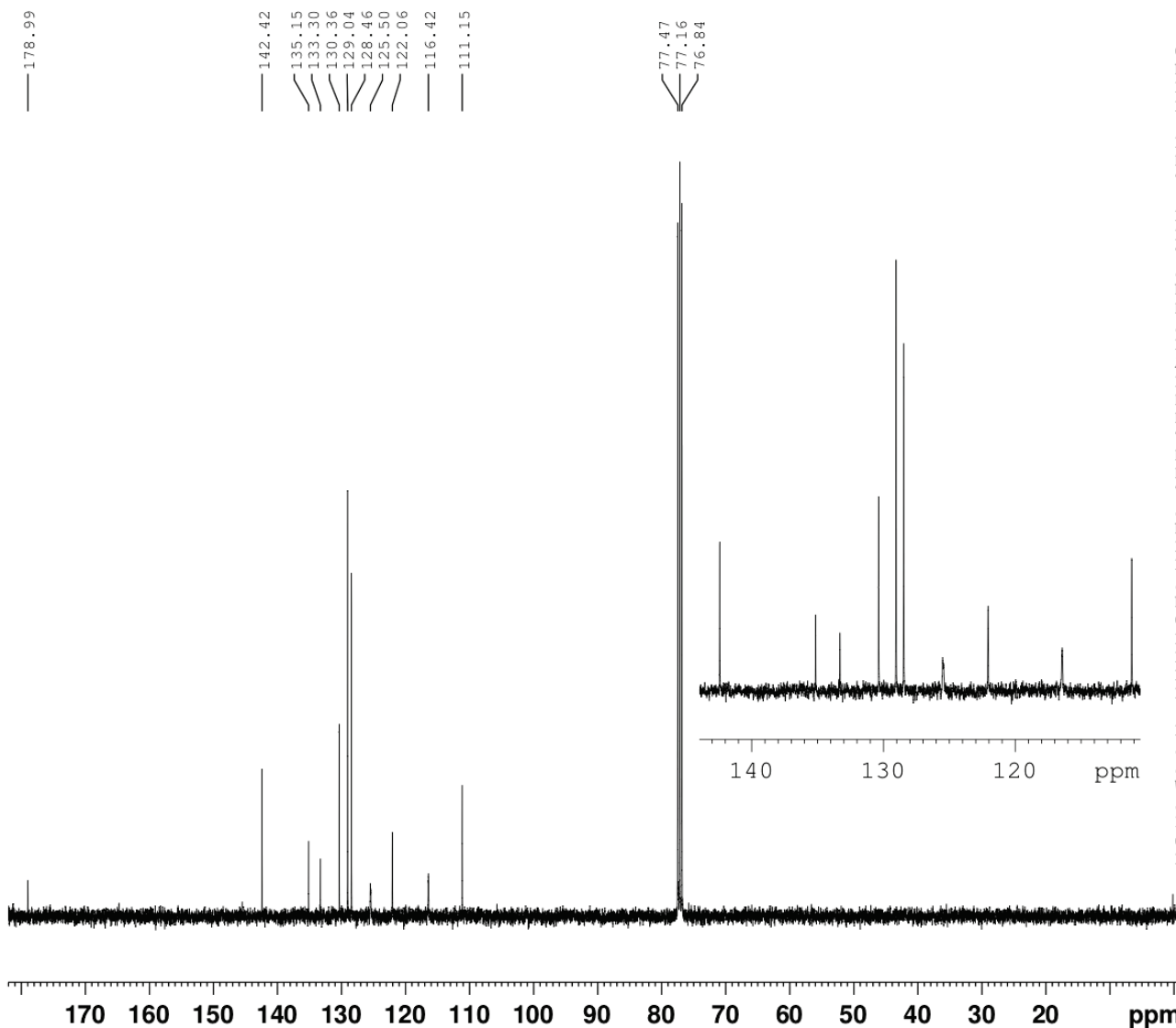
Current Data Parameters  
NAME Kpr2-Aph1  
EXPNO 10  
PROCNO 1

F2 - Acquisition Parameters  
Date\_ 20190604  
Time 15.47 h  
INSTRUM spect  
PROBHD Z108618\_0962 (  
PULPROG zg30  
TD 65536  
SOLVENT CDC13  
NS 16  
DS 2  
SWH 8012.820 Hz  
FIDRES 0.244532 Hz  
AQ 4.0894465 sec  
RG 143.16  
DW 62.400 usec  
DE 6.50 usec  
TE 294.2 K  
D1 1.00000000 sec  
TD0 1  
SFO1 400.2624716 MHz  
NUC1 1H  
P1 14.00 usec  
PLW1 11.72999954 W

F2 - Processing parameters  
SI 65536  
SF 400.2600104 MHz  
WDW EM  
SSB 0  
LB 0.30 Hz  
GB 0  
PC 1.00

Figure S4- <sup>1</sup>H NMR of (*E*)-3-phenyl-1-(1*H*-pyrrol-2-yl)prop-2-en-1-one.

<sup>13</sup>C; Kpr2-Aph1



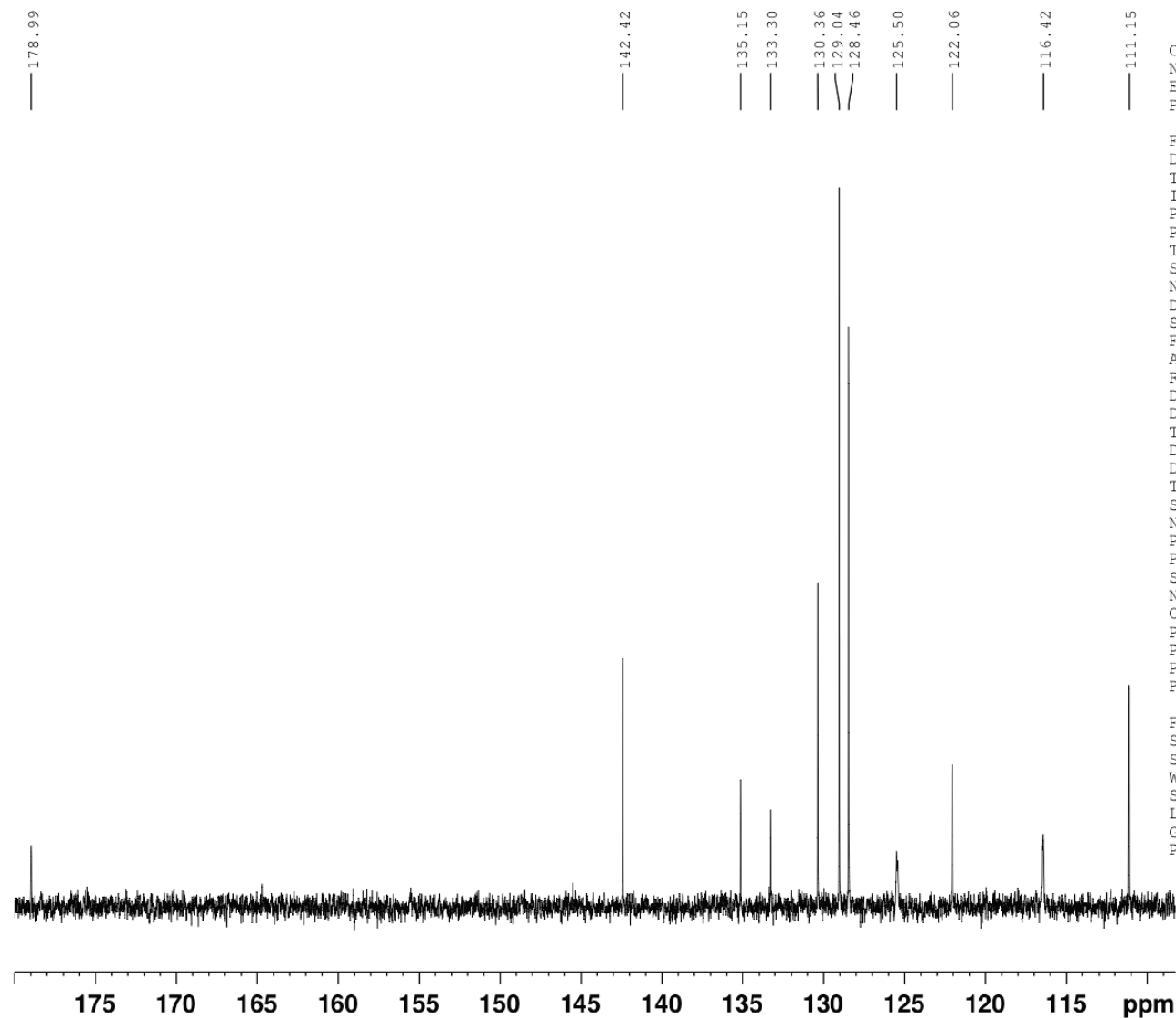
Current Data Parameters  
NAME Kpr2-Aph1  
EXPNO 11  
PROCNO 1

F2 - Acquisition Parameters  
Date\_ 20190604  
Time 15.56 h  
INSTRUM spect  
PROBHD Z108618\_0962 (  
PULPROG zgpg30  
TD 65536  
SOLVENT CDC13  
NS 128  
DS 4  
SWH 24038.461 Hz  
FIDRES 0.733596 Hz  
AQ 1.3631488 sec  
RG 202.4  
DW 20.800 usec  
DE 6.50 usec  
TE 295.1 K  
D1 2.0000000 sec  
D11 0.0300000 sec  
TD0 1  
SFO1 100.6555216 MHz  
NUC1 13C  
P1 10.00 usec  
PLW1 48.63600159 W  
SFO2 400.2616010 MHz  
NUC2 1H  
CPDPRG[2] waltz16  
PCPD2 90.00 usec  
PLW2 11.72999954 W  
PLW12 0.28382999 W  
PLW13 0.14275999 W

F2 - Processing parameters  
SI 32768  
SF 100.6454457 MHz  
WDW EM  
SSB 0  
LB 1.00 Hz  
GB 0  
PC 1.40

Figure S5- <sup>13</sup>C NMR of (*E*)-3-phenyl-1-(1*H*-pyrrol-2-yl)prop-2-en-1-one.

<sup>13</sup>C; Kpr2-Aph1



Current Data Parameters  
NAME Kpr2-Aph1  
EXPNO 11  
PROCNO 1

F2 - Acquisition Parameters  
Date\_ 20190604  
Time 15.56 h  
INSTRUM spect  
PROBHD Z108618\_0962 (  
PULPROG zgpg30  
TD 65536  
SOLVENT CDC13  
NS 128  
DS 4  
SWH 24038.461 Hz  
FIDRES 0.733596 Hz  
AQ 1.3631488 sec  
RG 202.4  
DW 20.800 usec  
DE 6.50 usec  
TE 295.1 K  
D1 2.0000000 sec  
D11 0.0300000 sec  
TD0 1  
SFO1 100.6555216 MHz  
NUC1 13C  
P1 10.00 usec  
PLW1 48.63600159 W  
SFO2 400.2616010 MHz  
NUC2 1H  
CPDPRG[2] waltz16  
PCPD2 90.00 usec  
PLW2 11.72999954 W  
PLW12 0.28382999 W  
PLW13 0.14275999 W

F2 - Processing parameters  
SI 32768  
SF 100.6454457 MHz  
WDW EM  
SSB 0  
LB 1.00 Hz  
GB 0  
PC 1.40

**Figure S6-** <sup>13</sup>C NMR of (*E*)-3-phenyl-1-(1*H*-pyrrol-2-yl)prop-2-en-1-one in the range 108 – 180 ppm.

#### 4- Crystal growth results via slow evaporation

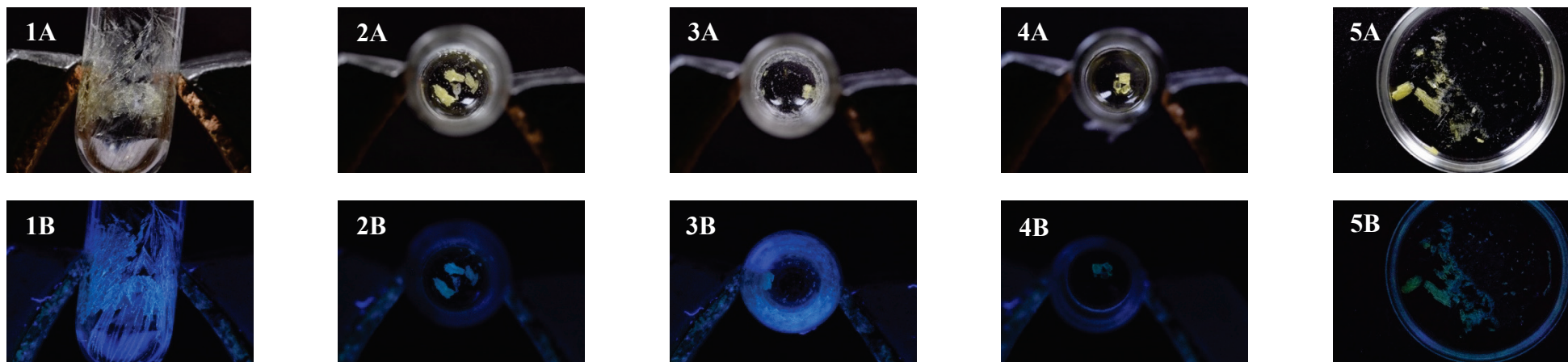


**Figure S7-** Images of (*E*)-1-(1*H*-pyrrol-2-yl)-3-(thiophen-2-yl)prop-2-en-1-one crystals that were grown by the slow evaporation process from a number of different solvents. All the solutions used had a concentration of  $0.05 \text{ mol dm}^{-3}$ . 1: Ethyl acetate; 2: THF; 3: Chloroform; 4: Methanol, 5: Acetone. Row A are pictures taken under visible light and row B are pictures taken under a UV lamp. Camera settings for row B – ISO: 1600, Shutter speed: 30 seconds, aperture: 40.0.

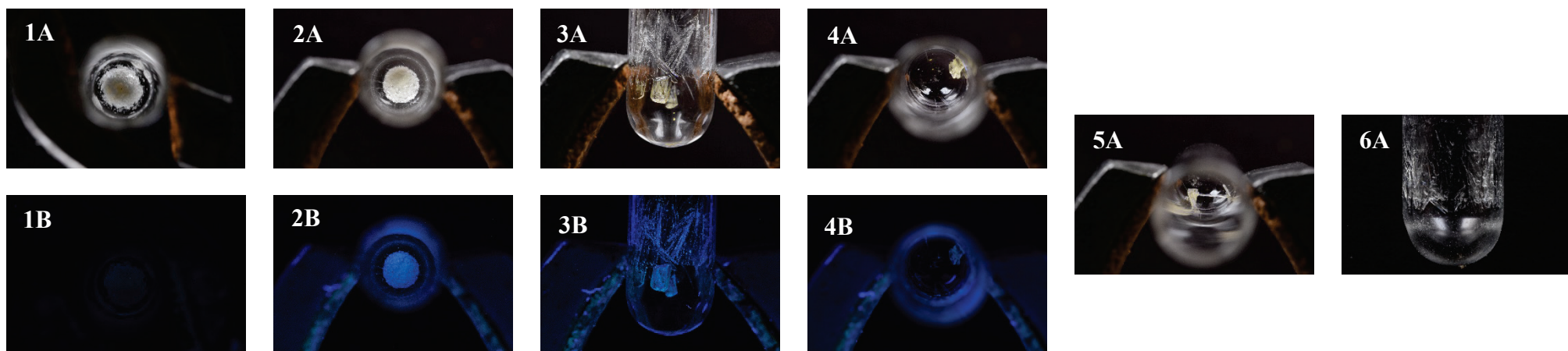
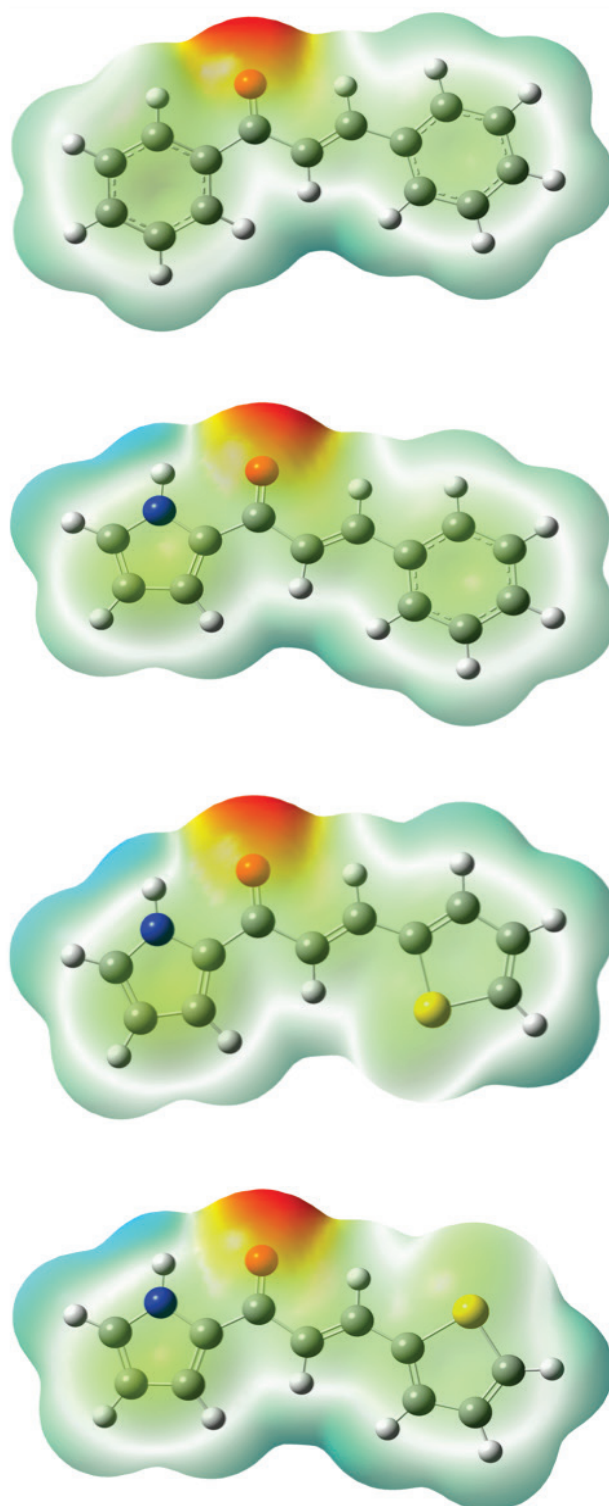


**Figure S8-** Images of (*E*)-3-phenyl-1-(1*H*-pyrrol-2-yl)prop-2-en-1-one crystals that were grown by the slow evaporation process from a number of different solvents. All the solutions used had a concentration of  $0.05 \text{ mol dm}^{-3}$ . 1: Ethyl acetate; 2: THF; 3: Methanol; 4: Acetone; 5: Chloroform; 6: Toluene. Row A are pictures taken under visible light and row B are pictures taken under a UV lamp. Camera settings for row B – ISO: 1600, Shutter speed: 30 seconds, aperture: 40.0.

## 5- Molecular electrostatic potential (MEP) plots

Molecular electrostatic potentials for the chalcones were plotted in GaussView 5.0.8 after optimisation of the structures using the B3LYP functional and 6-31G basis set (Frisch *et al.*, 2009)



$-6.500e-2$

$6.500e-2$

**Figure S9:** The MEP's for the three chalcones being considered in the range  $-6.5 \times 10^{-2}$  to  $6.5 \times 10^{-2}$  with an isovalue, MO = 0.020000, density = 0.000400. Top to Bottom: *Trans*-chalcone; (*E*)-3-phenyl-1-(1*H*-pyrrol-2-yl)prop-2-en-1-one; (*E*)-1-(1*H*-pyrrol-2-yl)-3-(thiophen-2-yl)prop-2-en-1-one (major component); (*E*)-1-(1*H*-pyrrol-2-yl)-3-(thiophen-2-yl)prop-2-en-1-one (minor component).

## 6- Differential Scanning Calorimetry

The DSC experiments involved cooling and heating the heterocyclic chalcones in hermetic aluminium pans between 200 °C to 0 °C at a rate of 10 °C min<sup>-1</sup>, using a TA instruments DSC 25 instrument under a dry nitrogen purge. *Trans*-chalcone was heated on a cycle between 100 °C to -50 °C at a rate of 10 °C min<sup>-1</sup>.

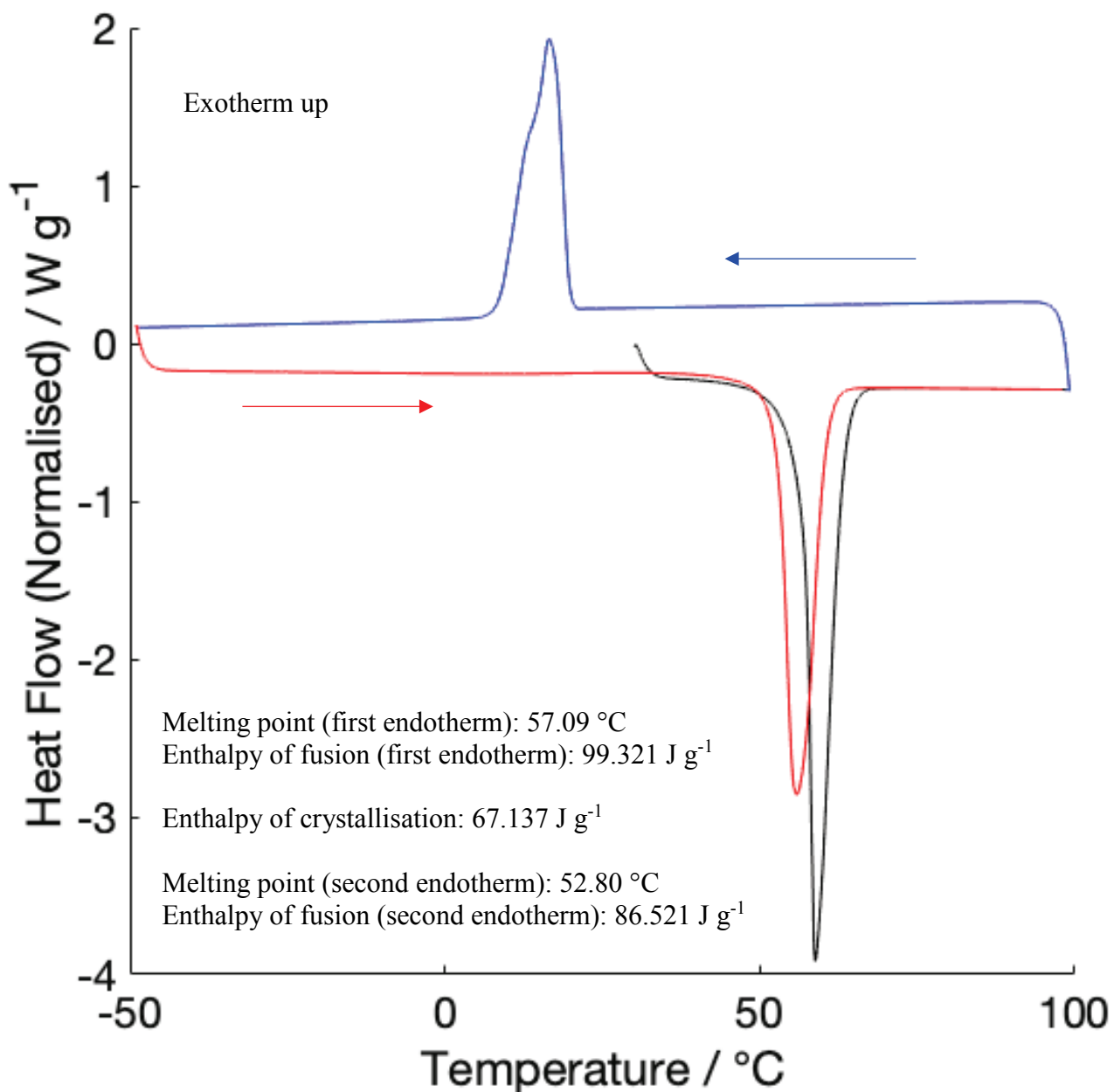


**Figure S10-** DSC heating and cooling cycle for *trans*-chalcone. Black line: Heating on cycle 1; Blue line: Cooling; Red line: Heating on cycle 2. Enthalpy of fusion for both endotherms and the enthalpy of crystallisation are provided, along with the melting points which were found. The mass of chalcone used was 10.1 mg (48 μmol).

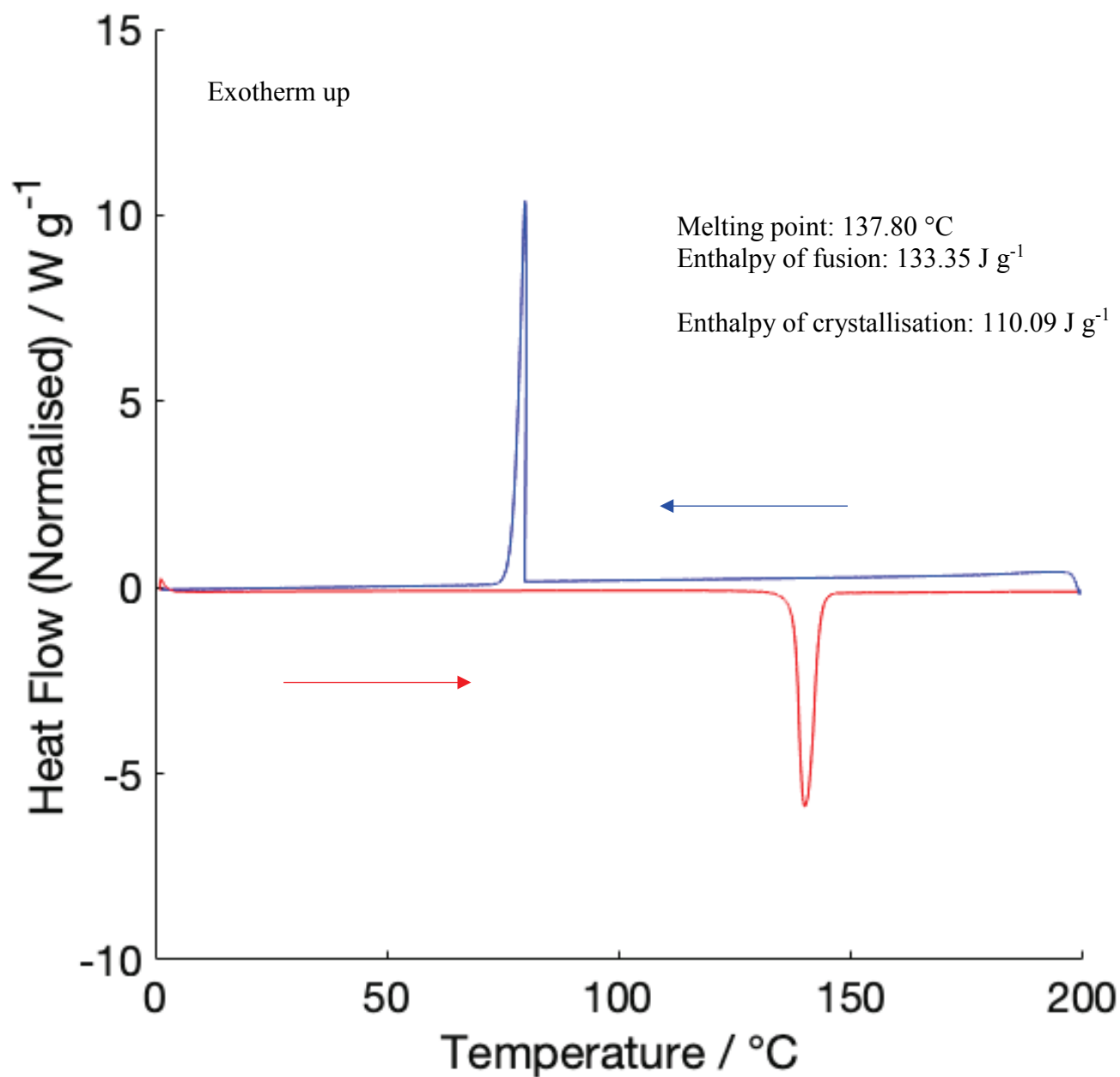


**Figure S11**- DSC heating and cooling cycle for (*E*)-3-phenyl-1-(1*H*-pyrrol-2-yl)prop-2-en-1-one. Blue line: Cooling; Red line: Heating. Enthalpy of fusion and crystallisation are provided along with the melting point. The mass of chalcone used was 2.4 mg (12 μmol).



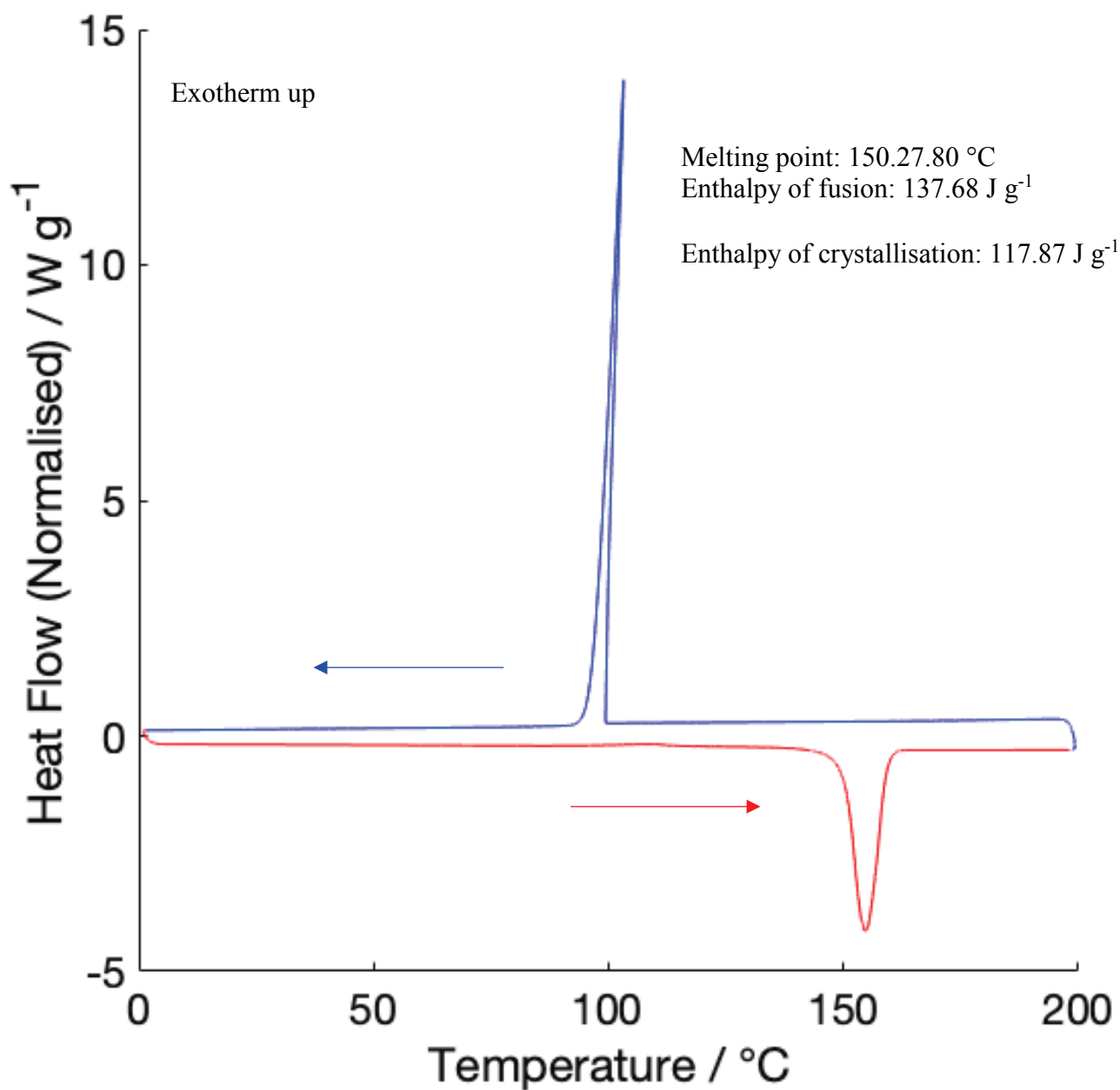


**Figure S12-** DSC heating and cooling cycle for (*E*)-1-(1*H*-pyrrol-2-yl)-3-(thiophen-2-yl)prop-2-en-1-one. Blue line: Cooling; Red line: Heating. Enthalpy of fusion and crystallisation are provided along with the melting point. The mass of chalcone used was 7.6 mg (37 μmol)



## 7- Powder X-ray diffraction data

Powder X-ray diffraction data was collected on a Bruker D8 Advance with Cu-K  $\alpha$  radiation ( $\lambda = 1.540600 \text{ \AA}$ ) and a PSD LynxEye detector, in Bragg-Brentano geometry. Data was collected over a  $2\theta$  range of  $5\text{-}50^\circ$  with a  $0.013^\circ$  step size and 1 second per step. The sample stage was not rotated. The simulated powder patterns obtained from the single crystal structures, using Mercury, matched the diffractograms collected and were used to assign the indices (Macrae *et al.*, 2006).

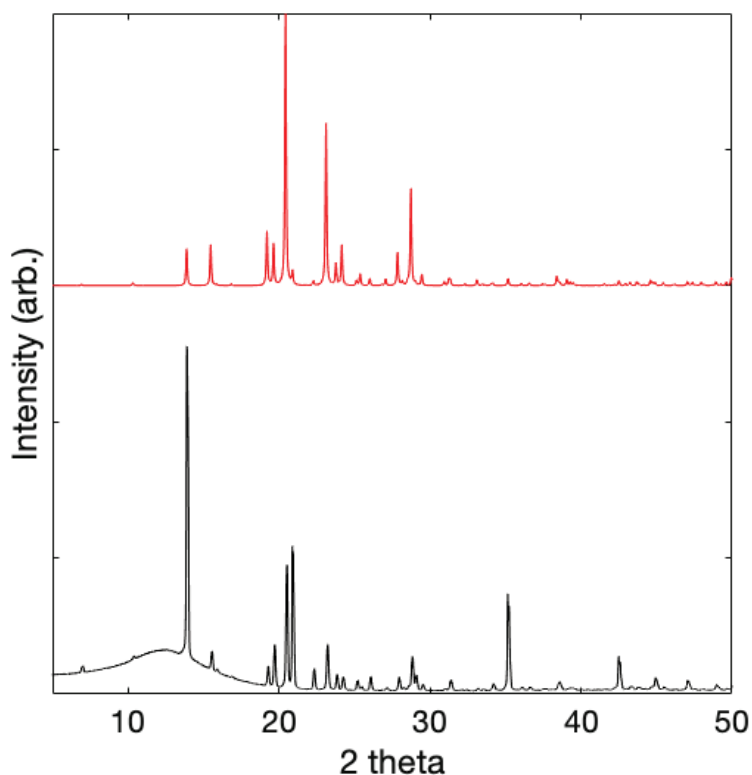


**Figure S13-** Comparison of the simulated powder X-ray pattern (red line) of *trans*-chalcone Form I to experimental data (black line).

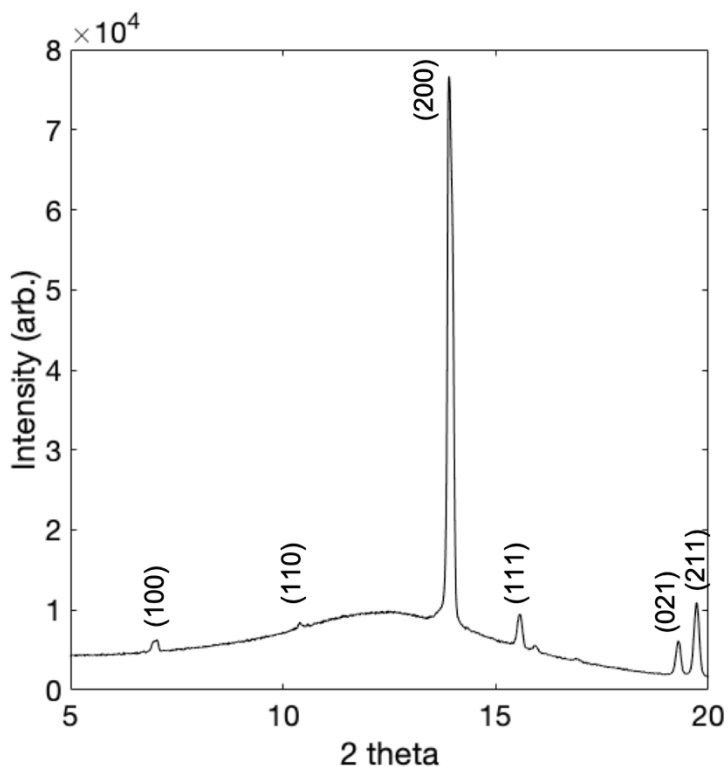


**Figure S14-** Powder X-ray diffraction data for *trans*-chalcone Form I in the range  $5^\circ 2\theta$  to  $20^\circ 2\theta$  with reflections indexed.

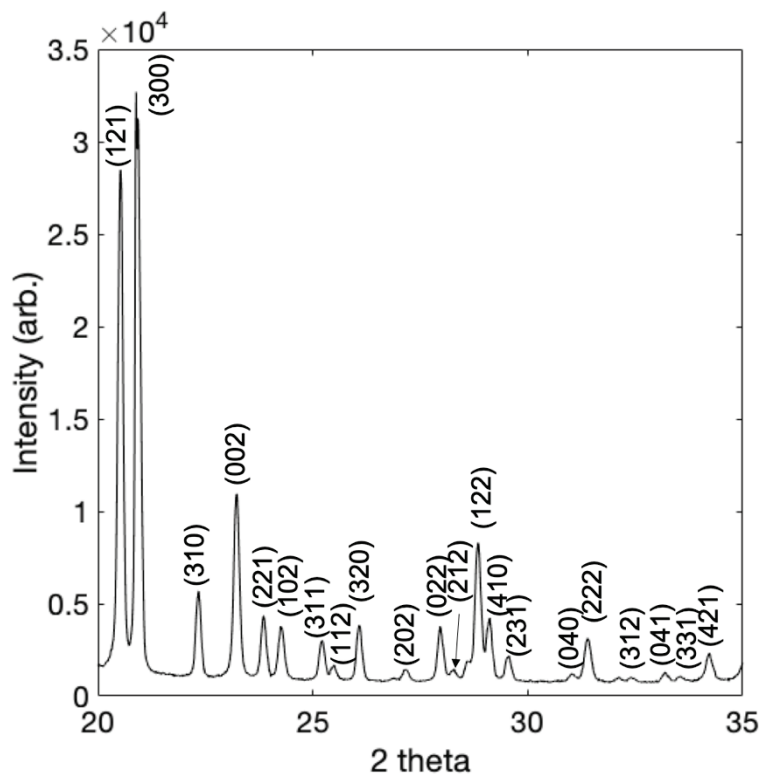


**Figure S15-** Powder X-ray diffraction data for *trans*-chalcone Form I in the range 20° 2θ to 35° 2θ with reflections indexed.

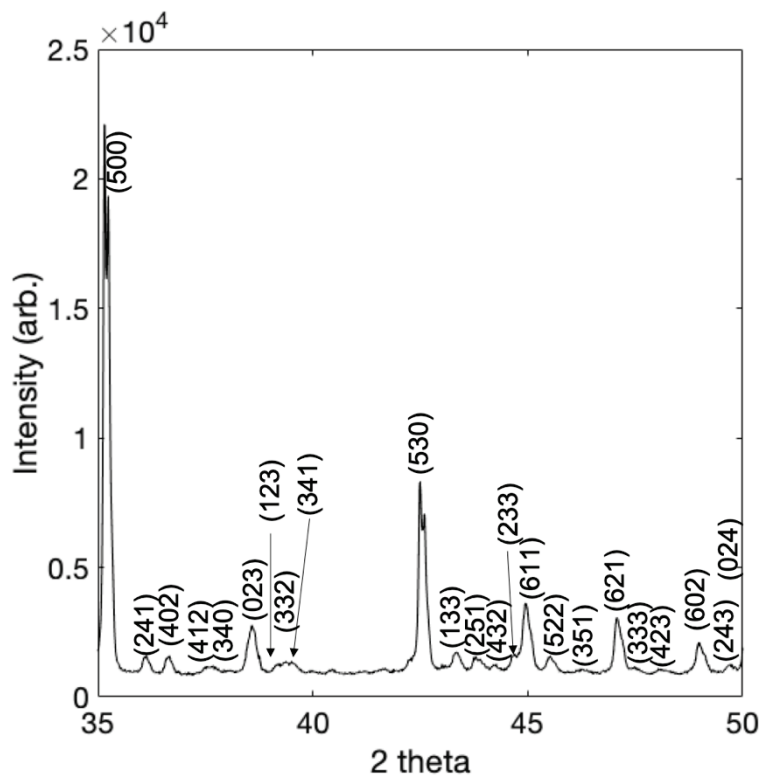


**Figure S16-** Powder X-ray diffraction data for *trans*-chalcone Form I in the range 35° 2θ to 50° 2θ with reflections indexed.

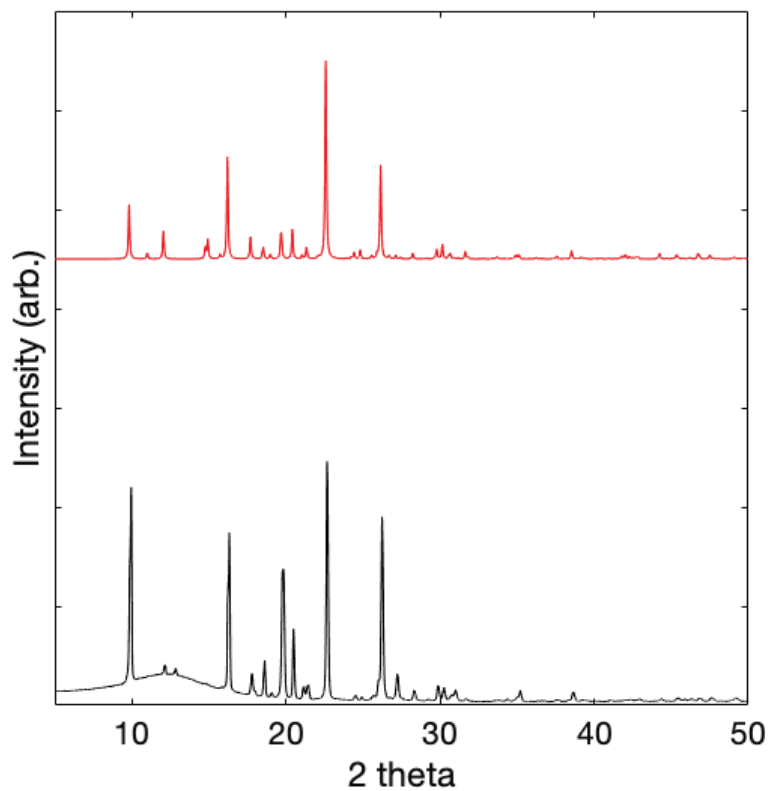


**Figure S17-** Comparison of the simulated powder X-ray pattern (red line) of *trans*-chalcone Form II to experimental data (black line).

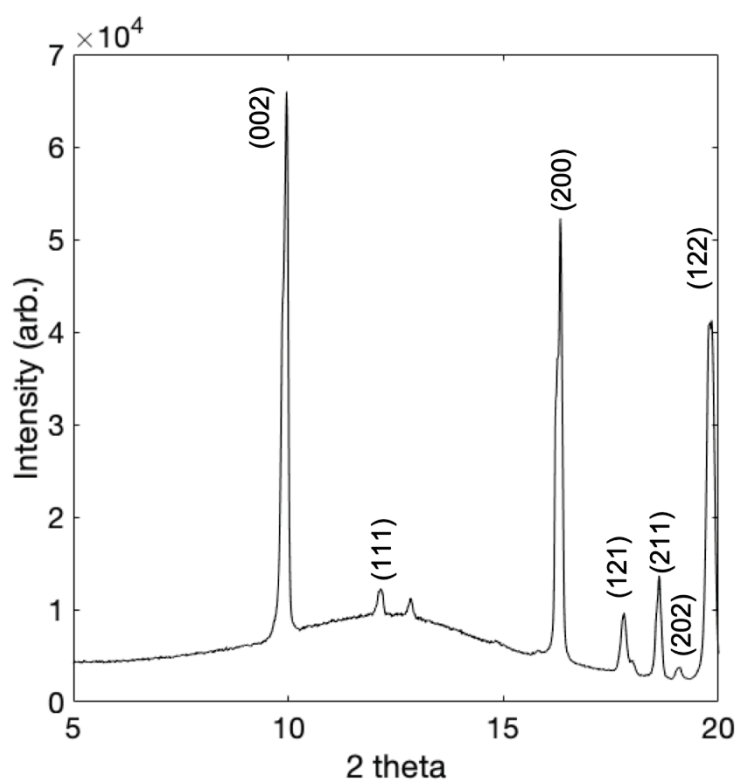


**Figure S18-** Powder X-ray diffraction data for *trans*-chalcone Form II in the range 5° 2θ to 20° 2θ with reflections indexed.

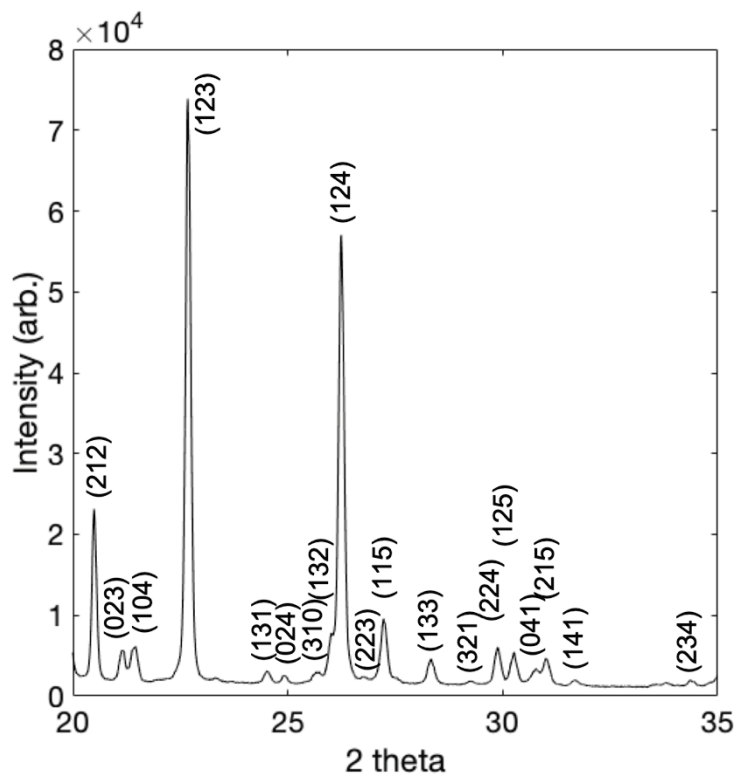


**Figure S19-** Powder X-ray diffraction data for *trans*-chalcone Form II in the range  $20^\circ 2\theta$  to  $35^\circ 2\theta$  with reflections indexed.

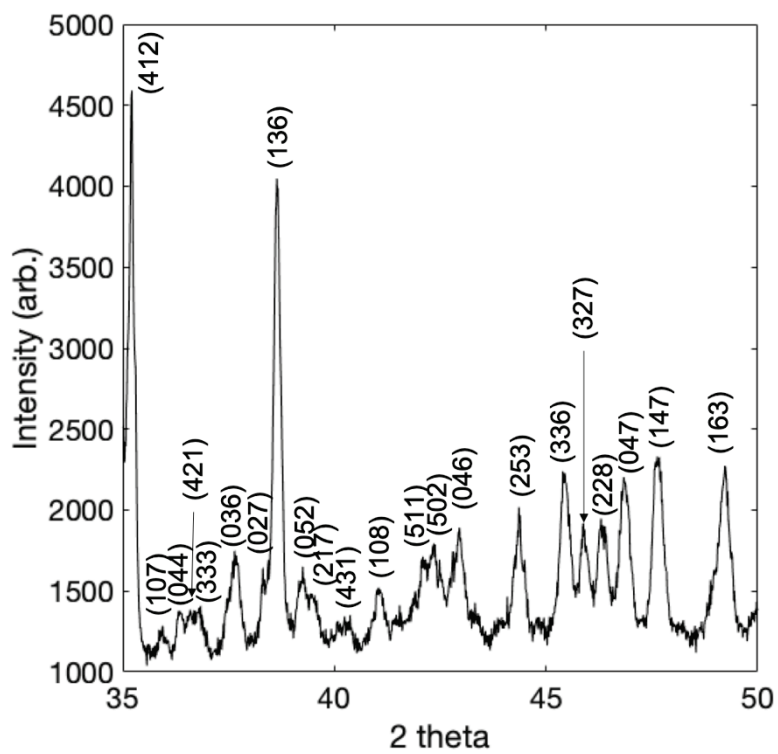


**Figure S20-** Powder X-ray diffraction data for *trans*-chalcone Form II in the range  $35^\circ 2\theta$  to  $50^\circ 2\theta$  with reflections indexed.

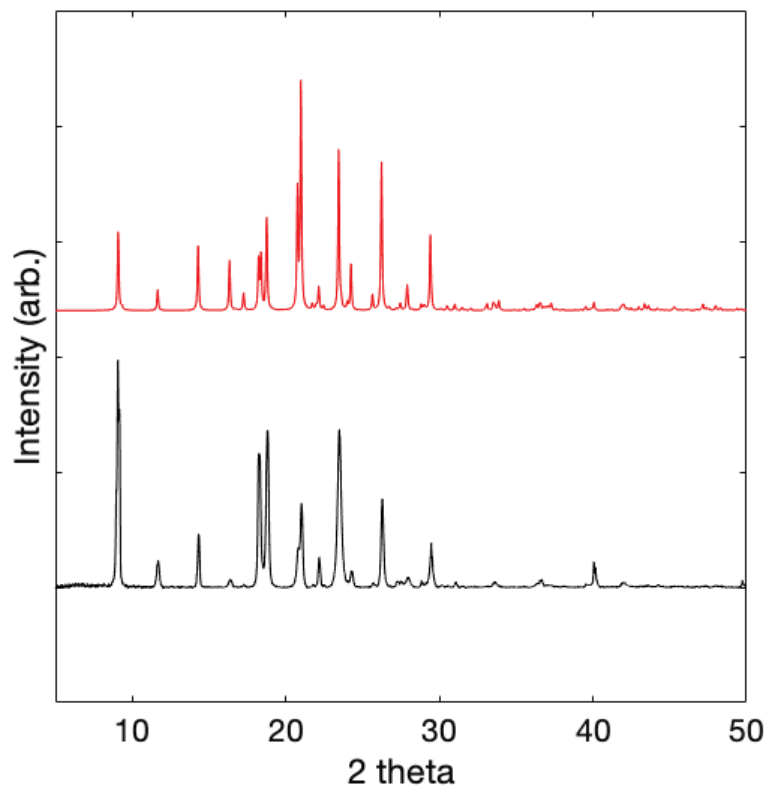


**Figure S21-** Comparison of the simulated powder X-ray pattern (red line) of (*E*)-3-phenyl-1-(1*H*-pyrrol-2-yl)prop-2-en-1-one to experimental data (black line).

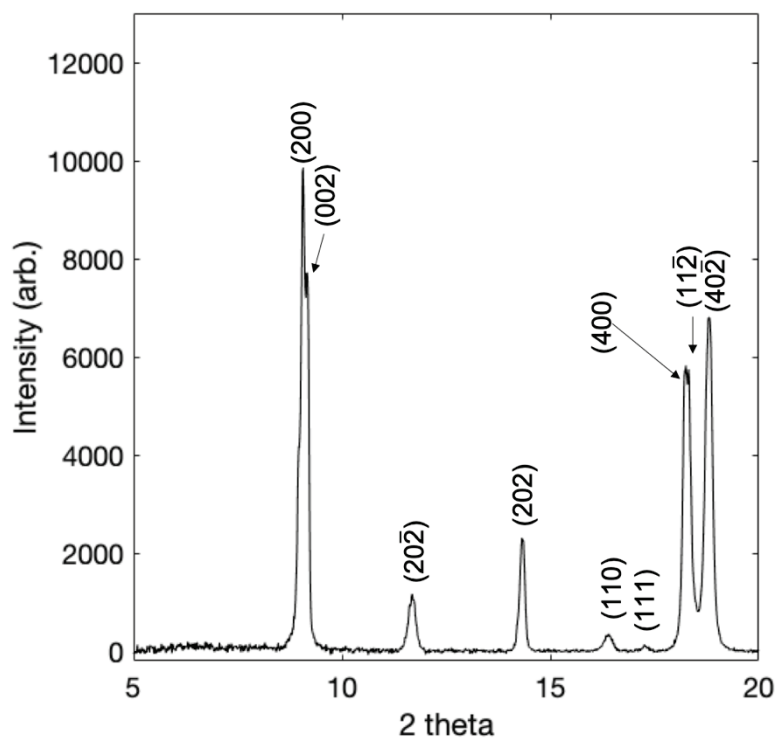


**Figure S22-** Powder X-ray diffraction data for (*E*)-3-phenyl-1-(1*H*-pyrrol-2-yl)prop-2-en-1-one in the range 5° 2θ to 20° 2θ with reflections indexed.

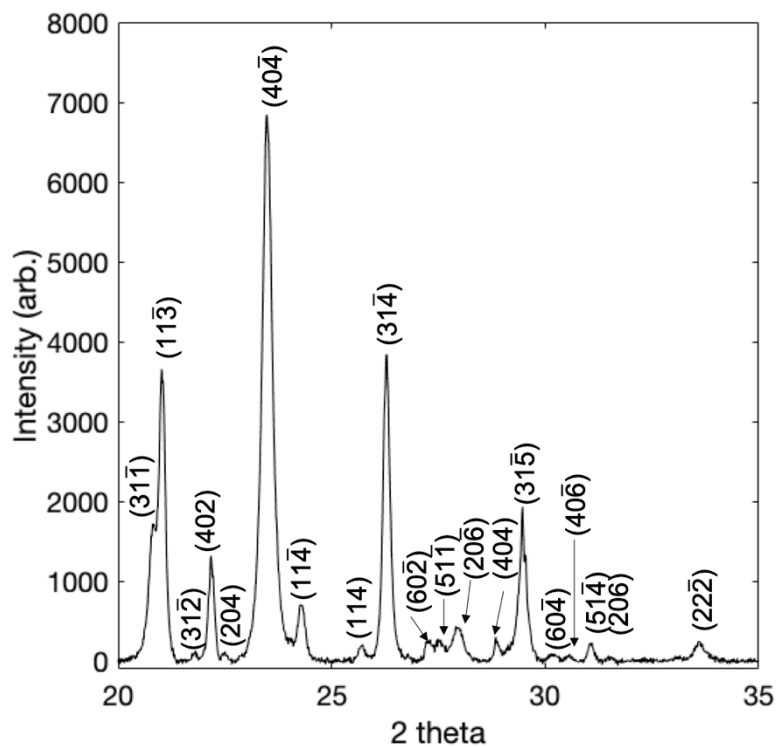


**Figure S23-** Powder X-ray diffraction data for (*E*)-3-phenyl-1-(1*H*-pyrrol-2-yl)prop-2-en-1-one in the range 20° 2θ to 35° 2θ with reflections indexed.

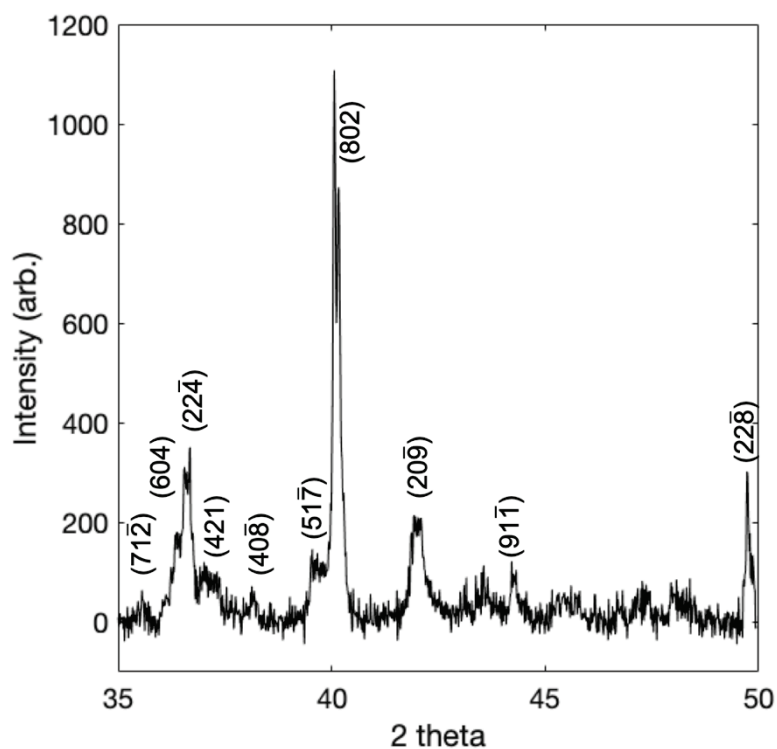


**Figure S24-** Powder X-ray diffraction data for (*E*)-3-phenyl-1-(1*H*-pyrrol-2-yl)prop-2-en-1-one in the range 35° 2θ to 50° 2θ with reflections indexed.

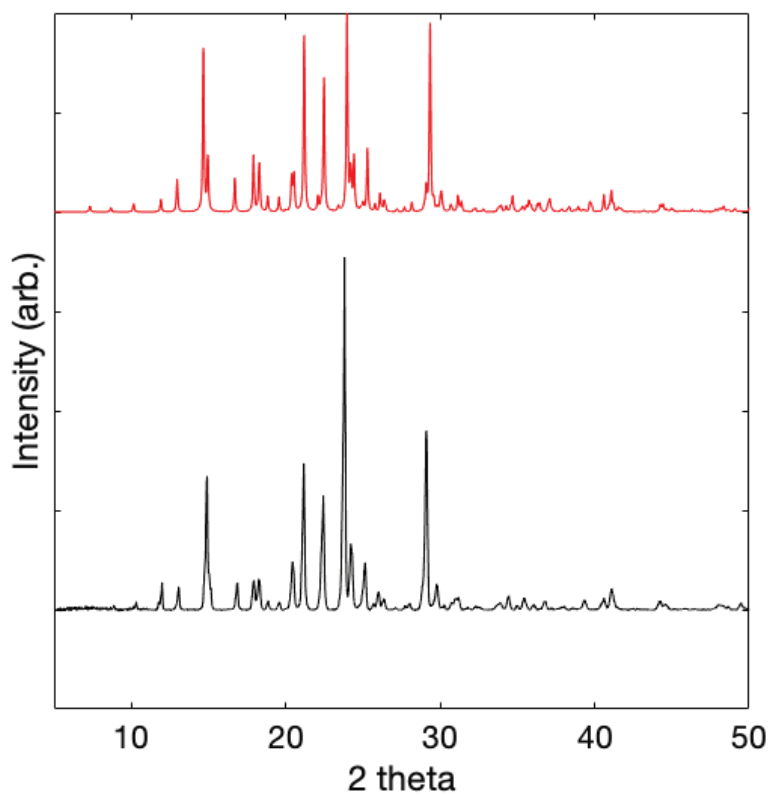


**Figure S25-** Comparison of the simulated powder X-ray pattern (red line) of (*E*)-1-(1*H*-pyrrol-2-yl)-3-(thiophen-2-yl)prop-2-en-1-one to experimental data (black line).

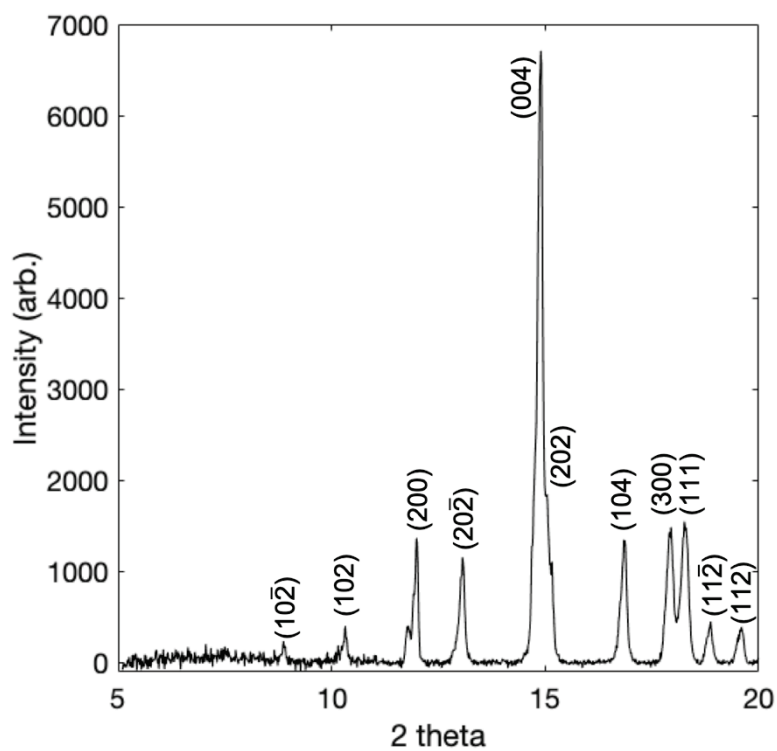


**Figure S26-** Powder X-ray diffraction data for (*E*)-1-(1*H*-pyrrol-2-yl)-3-(thiophen-2-yl)prop-2-en-1-one in the range 5° 2θ to 20° 2θ with reflections indexed.

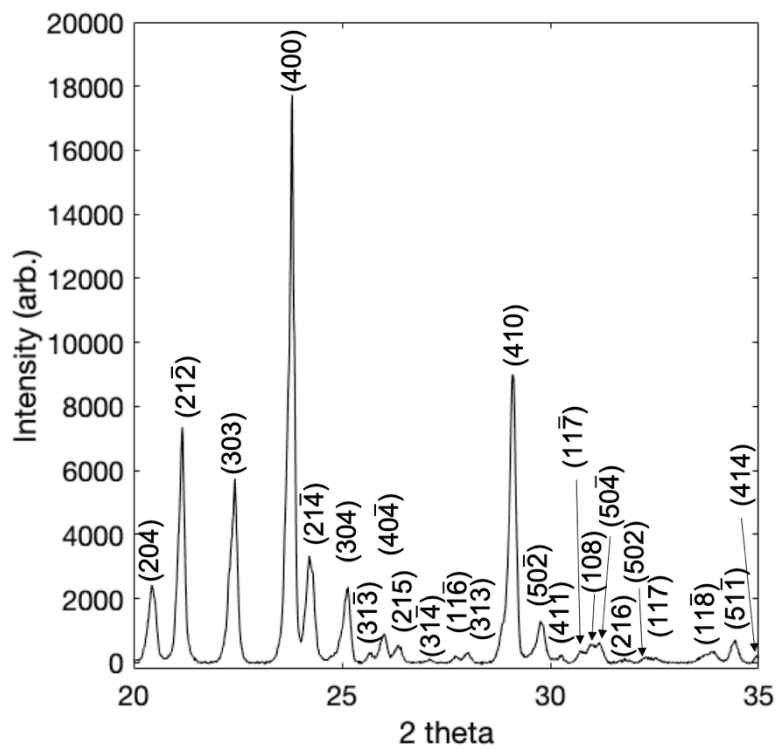


**Figure S27-** Powder X-ray diffraction data for *(E)*-1(1*H*-pyrrol-2-yl)-3-(thiophen-2-yl)prop-2-en-1-one in the range 20° 2θ to 35° 2θ with reflections indexed.

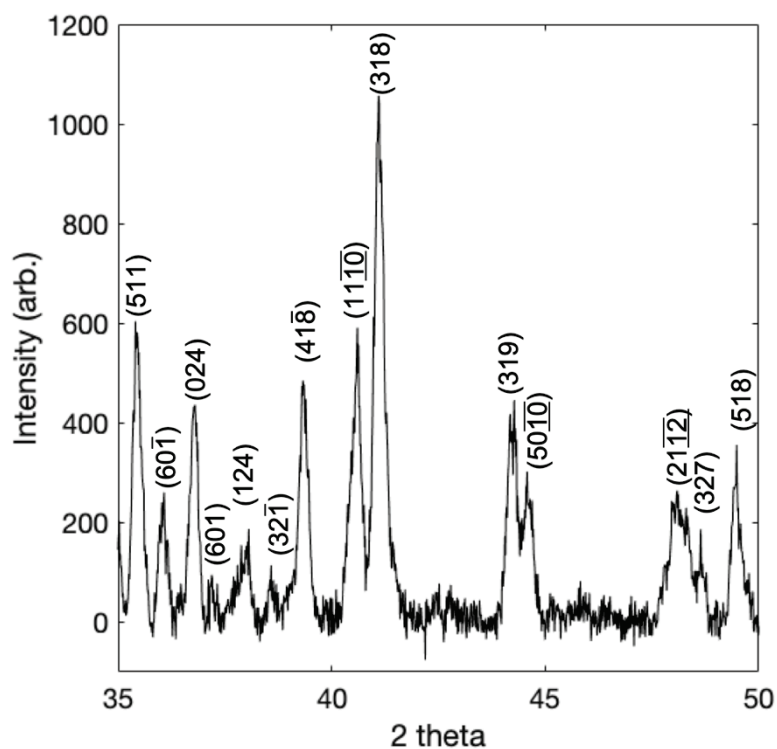


**Figure S28-** Powder X-ray diffraction data for *(E)*-1(1*H*-pyrrol-2-yl)-3-(thiophen-2-yl)prop-2-en-1-one in the range 35° 2θ to 50° 2θ with reflections indexed.



## 8- Single crystal X-ray diffraction data

Single crystals of C<sub>11</sub>H<sub>9</sub>NOS [(*E*)-1-(1*H*-pyrrol-2-yl)-3-(thiophen-2-yl)prop-2-en-1-one] were grown by slow evaporation from THF at a concentration of 0.05 mol dm<sup>-3</sup>.

Single crystal X-ray diffraction experiments were carried out at 100(2) K on a Bruker APEX II CCD diffractometer using Mo-K  $\alpha$  radiation ( $\lambda = 0.71073$  Å). Intensities were integrated and absorption corrections were based on equivalent reflections using SADABS (*SAIN*T+; Bruker, 2007; *SADABS*; Bruker, 2001). The structure was solved using Superflip and refined against F<sup>2</sup> in SHELXL using Olex2 (Palatinus and Chapuis, 2007; Palatinus *et al.*, 2012; Sheldrick, 2008; Sheldrick, 2015; Dolomanov *et al.*, 2009). Crystal structure and refinement data are given in Table S2.

The structure was refined as a 2-component non-merohedral twin. Hydrogen atoms on nitrogen atoms were found by difference map after all other atoms had been refined. All other hydrogen atoms were placed geometrically and refined using a riding model. Both molecules, in the asymmetric unit, contain a disordered thiophene group which has been modelled in two positions with a refined occupancy ratio of 0.922:0.078(2) in molecule 1 and 0.884:0.116(2) in molecule 2. Equivalent atom distances in the major and minor components (e.g. C1-C2 and C1A-C2A) have been restrained to be the same. The ADPs of atoms in close proximity have also been restrained to be the same. Crystal figures were produced on Mercury 4.1.3 (Macrae *et al.*, 2006).

CCDC 1952662 contains the supplementary crystallographic data for this paper.

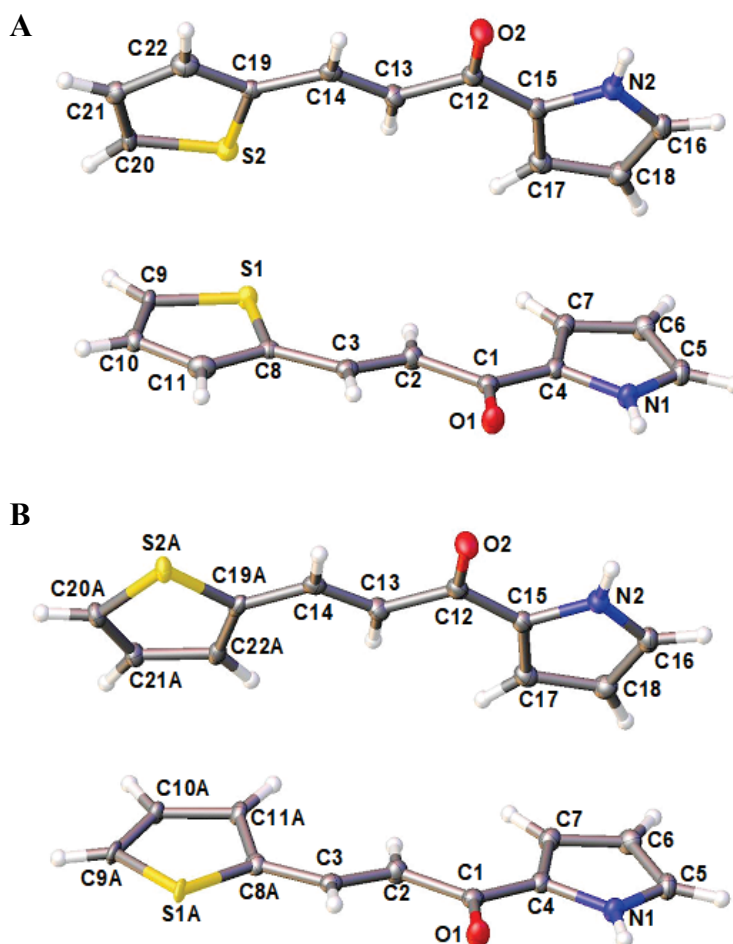


**Figure S29-** Diagrams of (*E*)-1-(1*H*-pyrrol-2-yl)-3-(thiophen-2-yl)prop-2-en-1-one showing the two disordered components separately. A: Major occupancy arrangement; B: Minor occupancy arrangement.

**Table S2-** Crystal data and structure refinement relating to (*E*)-1-(1*H*-pyrrol-2-yl)-3-(thiophen-2-yl)prop-2-en-1-one.

Empirical formula	C <sub>11</sub> H <sub>9</sub> NOS
Formula weight / g mol <sup>-1</sup>	203.25
Temperature / K	99.96
Crystal system	Monoclinic
Space Group	<i>P</i> 2 <sub>1</sub> / <i>c</i>
Hall Group	- <i>P</i> 2ybc
<i>a</i> / Å	15.0288(5)
<i>b</i> / Å	5.3086(2)
<i>c</i> / Å	24.4440(8)
$\alpha$ / °	90
$\beta$ / °	99.133(2)
$\gamma$ / °	90
Volume / Å <sup>3</sup>	1925.46(12)
<i>Z</i> , <i>Z'</i>	8, 2
$\rho_{\text{calc}}$ / g cm <sup>-3</sup>	1.402
$\mu$ / mm <sup>-1</sup>	0.298
<i>F</i> <sub>000</sub>	848.0
Crystal size / mm <sup>3</sup>	0.534 x 0.284 x 0.257
Radiation	Mo K $\alpha$ ( $\lambda$ = 0.71073 Å)
2 $\theta$ range for data collection	2.744 to 55.122
Index ranges	-19 ≤ <i>h</i> ≤ 19 0 ≤ <i>k</i> ≤ 6 0 ≤ <i>l</i> ≤ 31
Reflections collected	6848
Independent reflections	6848 [ <i>R</i> <sub>sigma</sub> = 0.0295]
Data/restraints/ parameters	6848/312/354
Goodness-of-fit on <i>F</i> <sup>2</sup>	1.031
Final <i>R</i> indexes [ <i>I</i> ≥ 2 $\sigma$ ( <i>I</i> )]	<i>R</i> <sub>1</sub> = 0.0365, <i>wR</i> <sub>2</sub> = 0.0856
Final <i>R</i> indexes [all data]	<i>R</i> <sub>1</sub> = 0.0505, <i>wR</i> <sub>2</sub> = 0.0923
Targets diff. peak/hole / e Å <sup>-3</sup>	0.30 / -0.27

**Table S3-** Hydrogen bonds for (*E*)-1-(1*H*-pyrrol-2-yl)-3-(thiophen-2-yl)prop-2-en-1-one.

D	H	A	d(D-H) / Å	d(H-A) / Å	d(D-A) / Å	D-H-A / °
N1	H1B	O1 <sup>1</sup>	0.83(2)	2.05(2)	2.841(2)	160(2)
N2	H2B	O2 <sup>2</sup>	0.84(2)	2.03(2)	2.832(2)	158(2)

<sup>1</sup>2-X, 2-Y, 1-Z; <sup>2</sup>1-X, 3-Y, 1-Z

## **References**

Bruker (2001). *SADABS*. Bruker AXS Inc., Madison, Wisconsin, USA.

Bruker (2007). *SAINTE+ Integration Engine*. Bruker AXS Inc., Madison, Wisconsin, USA.

Dolomanov, O. V., Bourhis, L. J., Gildea, R. J., Howard, J. A. K. and Puschmann, H. (2009), *J. Appl. Crystallogr.*, **42**, 339-341.

Frisch, M. J. *et al.* (2009). *GAUSSIAN09*. Gaussian Inc., Wallingford, CT, USA.

Macrae, C. F., Edgington, P. R., McCabe, P., Pidcock, E., Shields, G. P., Taylor, R., Towler, M. & van de Streek, J. (2006). *J. Appl. Cryst.* **39**, 453-457.

Palatinus, L. and Chapuis, G. (2007), *J. Appl. Crystallogr.*, **40**, 786-790.

Palatinus, L., Prathapa, S. J. and van Smaalen, S. (2012), *J. Appl. Crystallogr.*, **45**, 575-580.

Reichardt, C. and Welton, T. (2011). 4<sup>th</sup> ed., *Solvents and Solvent Effects in Organic Chemistry*, Wiley-VCH publishers.

Sheldrick, G. M. (2008) *Acta Crystallogr. A: Found. Crystallogr.*, **64**, 112-122.

Sheldrick, G. M. (2015) *Acta Crystallogr. C*, **71**, 3-8.